Topologically Constrained Manganese(III) and Iron(III) Complexes of Two Cross-Bridged Tetraazamacrocycles

Timothy J. Hubin,[†] James M. McCormick,[†] Nathaniel W. Alcock,[‡] and Daryle H. Busch*,[†]

Chemistry Departments, The University of Kansas, Lawrence, Kansas 66045, and
The University of Warwick, Coventry CV4 7AL, England

Received October 18, 1999

A family of Mn^{3+} and Fe^{3+} complexes of 4,11-dimethyl-1,4,8,11-tetraazabicyclo[6.6.2]hexadecane (**1**) and 4,-10-dimethyl-1,4,7,10-tetraazabicyclo[5.5.2]tetradecane (**2**) has been prepared by the chemical oxidation of the divalent manganese and iron analogues. The ligands are ethylene cross-bridged tetraazamacrocycles derived from cylam and cyclen, respectively. The synthesis and characterization of these complexes, including X-ray crystal structure determinations, are described. The structural evidence demonstrates that the tetradentate ligands enforce distorted octahedral geometries on the metal ions, with two *cis* sites occupied by labile ligands. Magnetic measurements reveal that the complexes are high spin with typical magnetic moments. Cyclic voltammetry shows reversible redox processes for the Fe^{3+}/Fe^{2+} couples of the iron(III) complexes, while Mn^{3+}/Mn^{2+} and Mn^{4+}/Mn^{3+} couples were observed for the complexes with manganese(III). The manganese chemistry of **1** was studied in depth. The dichloro manganese(III) cation of **1** undergoes facile ligand substitution reactions at the labile, monodentate sites, for example substituting azide for chloride ligands. Air oxidation of the dichloro complex of Mn $(\mathbf{1})^{2+}$ in basic solution does not give the expected μ-oxo dimeric product common to manganese. Instead, an unusual manganese(III)−OH complex has been isolated from this reaction and structurally characterized. A similar reaction under slightly different conditions gives a putative $Mn^{III}(OH)_2$ complex that metathesizes to $Mn^{III}(OMe)_2$ upon recrystallization from methanol.

Introduction

The thermodynamic sink represented by the mineral forms of manganese and iron oxides limits the utility, especially in aqueous media, of functional catalysts based on common ligands such as polyamines and polyethers.[1] Yet, in nature manganese and iron share with copper dominance over the vast realm of redox catalysis. Cytochrome P450,[2] catechol dioxygenase,[3] methane monooxygenase,[4] and lipoxygenase[5] display the power and selectivity found in natural iron-based oxidation catalysis while Mn catalase,[6] mitochondrial superoxide dismutase,[7] and photosystem II[8] similarly illustrate the potency of manganese derivatives. In biomimicry, *N*,*N*′,*N*″-trimethyl-1,4,7-triazacyclononane, Me_3[9]aneN3, provides an example of manganese and iron complexes in which some solubility is retained and the manganese complex is a potent oxidation catalyst.[9] A principal feature of this and other catalysts having common nitrogen donors and vacant coordination sites is their tendency to form dimers in which higher valent metal ions are present.

We have hypothesized that the principles of modern coordination chemistry[10] should allow us to design ligands that would be strikingly resistant to oxidative hydrolysis while still having available sites for direct binding of the metal ion to either a terminal oxidant or substrate or both. We envision that kinetically stable, mononuclear manganese and iron complexes that are not coordinatively saturated by their stabilizing ligand are also capable of supporting higher-valent metal ions. It is well-known today that, given good complementarity and the same donor atoms, both the thermodynamic and kinetic stabilities of metal complexes increase in the series monodentate ligand < linear or branched chelating ligand < macrocyclic ligand <

* Corresponding author.
[†] The University of Kansas.
[‡] The University of Warwick.

(1) Cotton, F. A.; Wilkinson, G. *Advanced Inorganic Chemistry*, 5th ed.; Wiley & Sons: New York, 1988.
(2) Ortiz de Montellano, P. R. Ed. *Cytochrome P450: Structure, Mechanism, and Biochemistry*; Plenum Press: New York, 1986.
(3) (a) Jang, H. G.; Cox, D. D.; Que, L., Jr. *J. Am. Chem. Soc.* **1991**, *113*, 9200. (b) Han, S.; Eltis, L. D.; Timmis, K. N.; Muchmore, S. W.; Bolin, J. T. *Science* **1995**, *270*, 976.
(4) (a) Waller, B. J.; Lipscomb, J. D. *Chem. Rev.* **1996**, *96*, 2625. (b) Rosenzweig, A. C.; Nordlund, P.; Takahara, P. M.; Frederich, C. A.; Lippard, S. J. *Chem. Biol.* **1995**, *2*, 409. (c) Que, L., Jr.; Dong, Y. *Acc. Chem. Res.* **1996**, *29*, 190.
(5) Boyington, J. C.; Gaffney, B. J.; Amzel, L. M. *Science* **1993**, *260*, 1482.
(6) (a) Pecoraro, V. L., Ed. *Manganese Redox Enzymes*; VCH: New York, 1992. (b) Vainshtein, B. K.; Melik-Adayamyan, W. R.; Barynin, V. V.; Vagin, A. A.; Grebenko, A. I. *Proc. Int. Symp. Biomol. Struct. Interact., Suppl. J. Biosci.* **1985**, *8*, 471. (c) Barynin, V. V.; Vagin, A. A.; Melik-Adayamyan; W. R.; Grebenko, A. I.; Khangulov, S. V.; Popov, A. N.; Andrianova, M. E.; Vainshtein, B. K. *Dokl. Akad. Nauk SSSR* **1986**, *228*, 877. (d) Weighardt, K.; *Angew. Chem., Int. Ed. Engl.* **1989**, *28*, 1153.
(7) (a) Ludwig, M. L.; Metzger, A. L.; Pattridge, K. A.; Stallings, W. C. *J. Mol. Biol.* **1991**, *219*, 335. (b) Borgstahl, G. E. O.; Parge, H. E.; Hickey, M. J.; Beyer, W. F., Jr.; Hallewell, R. A.; Tainer, J. A. *Cell* **1992**, *71*, 107.
(8) (a) Prosperpio, D. M.; Hoffman, R.; Dismukes, G. C. *J. Am. Chem. Soc.* **1992**, *114*, 4374. (b) Ono, T.; Noguchi, T.; Inoue, Y.; Kusunoki, M.; Matsushita, T.; Oyanagi, H. *Science* **1992**, *258*, 1335. (c) Bossek, U.; Weyhermüller, T.; Weighardt, K.; Nuber, B.; Weiss, J. *J. Am. Chem. Soc.* **1990**, *112*, 6387.
(9) (a) Wieghardt, K.; Bossek, U.; Nuber, B.; Weiss, J.; Bonvoisin, J.; Corbella, M.; Vitols, S. E.; Girerd, J. J. *J. Am. Chem. Soc.* **1988**, *110*, 7398. (b) Quee-Smith, V. C.; DelPizzo, L.; Jurellar, S. H.; Kershner, J. L.; Hage, R. *Inorg. Chem.* **1996**, *35*, 6461. (c) Koek, J. H.; Russel, S. W.; van der Wolf, L.; Hage, R.; Warnaar, J. B.; Spek, A. L.; Kershner, J.; DelPizzo, L. *J. Chem. Soc., Dalton Trans.* **1996**, 353. (d) De Vos, D. E.; Bein, T. *J. Organomet. Chem.* **1996**, *520*, 195.
(10) Busch, D. H. *Chem. Rev.* **1993**, *93*, 847.

10.1021/ic9912225 CCC: $20.00
Published on Web 01/04/2001

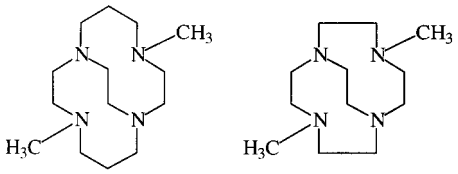

1 **2**

Figure 1. Recently reported cross-bridged ligands **1**[11a] and **2**[11b] used to prepare Fe^{3+} and Mn^{3+} complexes discussed in this paper.

macrobicyclic ligand, or cryptate. This sequence may be stated simply as follows: complex stability increases with the topological complexity of the ligand, given equal complementarity.[10] Specific organic molecules, that should possess the sought-after ligand properties, ethylene cross-bridged tetraazamacrocycles (Figure 1, structures **1** and **2**), were identified.[11] These tetradentate ligands are as topologically constrained as the macrobicyclic cryptates but, when bound, should leave labile coordination sites on the metal ion for further reaction. These molecules have already been synthesized in other laboratories,[11] but have not been fully exploited as ligands for transition metal complexes. We considered that the great rigidity of these short cross-bridged ligands, ethylene-bridged **1** and **2**, should impart enormous kinetic stability to their complexes,[10] and we have recently shown this to be the case for copper(II)[12] and manganese(II).[13] This kinetic stability confers on these transition metal complexes great promise in such applications as homogeneous catalysis, where complex stability has historically been a problem.

Attracted by the expectation of greatly diminished kinetic lability and enhanced thermodynamic stability, our goals were to develop synthetic methods for the introduction of metal ions into the highly basic ligand cleft and to explore the capabilities of the resulting complexes for biomimetic and catalytic applications. Attempts at the complexation of **1** and **2** with Fe^{2+} and Mn^{2+} salts in protic solvents or in aprotic solvents using hydrated metal salts were entirely unsuccessful.[12,14] This behavior was traced to the proton-sponge nature of the ligands. In water, the diprotonated form of free ligand **1** behaves as a monoprotic weak acid with pK_{a1} equal to 9.58(3), indicating that the second proton must be associated with a pK_{a2} value substantially greater than 13.[13] This obstacle was overcome by minimizing the activity of protons in the synthesis procedures. The Fe^{2+} and Mn^{2+} complexes of ligands **1** and **2** were prepared from the corresponding anhydrous complexes of the formula $M(py)_2Cl_2$, where py is pyridine, in dry CH_3CN.[13] We have previously reported the Fe^{2+} and Mn^{2+} complexes of **1** and **2** and their exciting chemical and physical properties.[13] Here, we discuss the chemical oxidation of those complexes to generate the Fe^{3+} and Mn^{3+} analogues and the characterization of these new, higher valent compounds. Studies revealing the reactivity of these complexes and their ability to withstand harsh aqueous conditions without decomposing or dimerizing are also presented. During these experiments, a rare mononuclear manganese(III)−OH complex was isolated and structurally characterized.

Experimental Section

NH_4PF_6 (95+%) and NaN_3 (99%) were purchased from Aldrich Chemical Co. Reagent grade Br_2 was purchased from Fisher. All solvents were of reagent grade and were dried, when necessary, by accepted procedures.[15]

Elemental analyses were performed by Quantitative Technologies Inc. or the Analytical Service of the University of Kansas. Mass spectra were measured by the Analytical Service of the University of Kansas on a VG ZAB HS spectrometer equipped with a xenon gun. The matrix used was NBA (nitrobenzyl alcohol).

Synthesis. The preparation of the $M(L)Cl_2$ (L = **1**, **2**, M = Mn^{2+}, Fe^{2+}) starting materials can be found elsewhere.[13]

[M(L)Cl$_2$]PF$_6$ (M = Mn^{3+}, Fe^{3+}; L = 1, 2). A dry methanol solution (20 mL) containing 0.001 mol of the appropriate $MLCl_2$ complex and 0.815 g (0.005 mol) of NH_4PF_6 was prepared under nitrogen. With stirring, 4−6 drops of Br_2 were added to the above solution, while a slow N_2 stream was maintained over it. Immediate precipitation of red-brown (manganese) or yellow-orange (iron) solids occurred in all cases. Stirring of the reaction mixture was continued for 15 min before nitrogen was bubbled through the solution in a fume hood for 30 min to remove excess Br_2. Full precipitation was realized after the sealed reaction mixtures were stored in a freezer overnight. Filtration on a glass frit, followed by washing with methanol and ether, gave the analytically pure products as the hexafluorophosphate salts of the $MLCl_2^+$ cations. Yield: 80−91%. [Fe(**1**)Cl$_2$]PF$_6$·0.5 H$_2$O: Anal. Calcd for $FeC_{14}H_{31}N_4Cl_2PF_6O_{0.5}$ C 31.42%, H 5.84%, N 10.47%. Found: C 31.18%, H 5.49%, N 10.10%. [Mn(**1**)Cl$_2$]PF$_6$: Anal. Calcd for $MnC_{14}H_{30}N_4Cl_2PF_6$: C 32.02%, H 5.76%, N 10.67%. Found: C 32.18%, H 5.74%, N 10.66%. [Fe(**2**)Cl$_2$]PF$_6$: Anal. Calcd for $FeC_{12}H_{26}N_4Cl_2PF_6$: C 28.94%, H 5.26%, N 11.25%. Found: C 28.60%, H 5.10%, N 11.02%. [Mn(**2**)Cl$_2$]PF$_6$: Anal. Calcd for $MnC_{12}H_{26}N_4Cl_2PF_6$: C 28.99%, H 5.27%, N 11.27%. Found: C 29.04%, H 5.10%, N 11.26%. FAB^+ mass spectra in methylene chloride (NBA matrix) exhibited peaks at $m/z = M(L)Cl_2^+$ for all four complexes. X-ray quality crystals of [Mn(**1**)Cl$_2$]PF$_6$ and [Mn(**2**)Cl$_2$]PF$_6$ were obtained by ether diffusion into acetone solutions.

[Mn(1)(N$_3$)$_2$]PF$_6$. To 0.442 g (0.841 mmol) of [Mn(**1**)Cl$_2$]PF$_6$ dissolved in 30 mL of dry acetonitrile was added 0.241 g (3.71 mmol) of NaN_3. The solution changed from red to orange and finally to brown over the period of several minutes. The reaction mixture was stirred overnight, at which point 1.0 g of KPF_6 was added and the solvent removed on a rotary evaporator. The brown residue was triturated with dry methylene chloride until the triturate was no longer deeply colored. The combined triturates were reduced in volume to ~15 mL and ether was added to afford a precipitate, which was collected by filtration. The product was washed with toluene and ether. After air-drying, 0.347 g (77%) of the product was obtained as an analytically pure, brown, microcrystalline powder. Anal. Calcd for $MnC_{14}H_{30}N_{10}PF_6$: C 31.23%, H 5.62%, N 26.02%. Found: C 31.03%, H 5.77%, N 26.02%. The FAB^+ mass spectrum in methylene chloride (NBA matrix) exhibited peaks at $m/z = 393$ (Mn(**1**)$(N_3)_2^+$) and $m/z = 351$ (Mn(**1**)$(N_3)^+$). X-ray quality crystals were obtained by the diffusion of ether into a methylene chloride solution.

[Mn(1)(OH)(OAc)]PF$_6$·NH$_4$OAc·NaCl. One-tenth gram (0.26 mmol) of Mn(**1**)Cl_2 was dissolved in 25 mL of 2 M NaOH, to which 5 mL of EtOH was then added. The solution immediately turned golden brown. Air was bubbled through the solution overnight, after which the mixture was filtered through Celite to remove traces of brown solids, and then 0.220 g (1 mmol) of NH_4PF_6 dissolved in 5 mL of water was added. The solution was then allowed to slowly evaporate in a crystallization dish in a fume hood. Over the course of 10 days, large clusters of very thin orange crystals slowly formed. These were collected by filtration and washed with a small amount of water. Yield: 106 mg, 61%. Anal. Calcd for $MnC_{18}H_{41}N_5O_5NaClPF_6$: C 32.47%, H 6.21%, N 10.52%. Found: C 32.66%, H 6.18%, N 10.65%. X-ray quality crystals were obtained by ether diffusion into a methanol solution to give the small brown crystals, solved as [Mn(**1**)(OH)(OAc)]PF$_6$ (omitting the coc-

(11) (a) Weisman, G. R.; Rogers, M. E.; Wong, E. H.; Jasinski, J. P.; Paight, E. S. *J. Am. Chem. Soc.* **1990**, *112*, 8604. (b) Bencini, A.; Bianchi, A.; Bazzicalupi, C.; Ciampolini, M.; Fusi, V.; Micheloni, M.; Nardi, N.; Paoli, P.; Valtancoli, B. *Supramol. Chem.* **1994**, *3*, 41.

(12) Hubin, T. J.; McCormick, J. M.; Collinson, S. R.; Alcock, N. W.; Busch, D. H. *Chem. Commun. (Cambridge)* **1998**, 1675.

(13) Hubin, T. J.; McCormick, J. M.; Collinson, S. R.; Perkins, C. M.; Alcock, N. W.; Kahol, P. K.; Raghunathan, A.; Busch D. H. *J. Am. Chem. Soc.* **2000**, *122*, 2512.

(14) (a) Weisman, G. R.; Wong, E. H.; Hill, D. C.; Rogers, M. E.; Reed, D. P.; Calabrese, J. C. *Chem. Commun. (Cambridge)* **1996**, 947. (b) Irving, H.; Williams, R. J. P. *J. Chem. Soc.* **1953**, *part III*, 3192.

(15) Perrin, D. D.; Armarego, W. L. F.; Perrin, D. R. *Purification of Laboratory Chemicals*, 2nd ed.; Pergamon Press: New York, 1980.

Table 1. Crystal Data and Structural Refinement Details

	[Mn(**2**)Cl_2]PF_6	[Mn(**1**)Cl_2]PF_6	[Mn(**1**)$(N_3)_2$]PF_6	[Mn(**1**)(OH)(OAc)]PF_6	[Mn(**1**)$(OMe)_2$]PF_6
formula	$MnC_{12}H_{26}N_4Cl_2PF_6$	$MnC_{14}H_{30}N_4Cl_2PF_6$	$MnC_{14}H_{30}N_{10}PF_2$	$MnC_{16}H_{33}N_4O_3PF_6$	$MnC_{16}H_{36}N_4O_2PF_6$
fw	497.18	525.23	538.39	529.37	516.40
cryst syst	monoclinic	orthorhombic	monoclinic	monoclinic	monoclinic
space group	$P2_1/n$	$Pna2_1$	$C2/c$	$P2_1/n$	$C2/c$
a (Å)	8.34030(10)	25.9253(10)	10.3187(5)	8.9002(7)	11.8650(10)
b (Å)	19.9211(4)	8.4401(3)	14.418(2)	15.6033(12)	12.7480(10)
c (Å)	12.15580(10)	9.5545(4)	15.129(2)	16.5950(12)	14.8378(5)
β (deg)	95.4620(10)	90	100.604(3)	101.8420(10)	96.544(5)
V (Å^3)	2010.49(5)	2090.64(14)	2212.4(4)	2255.5(3)	2229.7(3)
Z	4	4	4	4	4
ρ_{calc} (g/cm^3)	1.643	1.669	1.616	1.559	1.538
temp (K)	180(2)	180(2)	200(2)	210(2)	200(2)
abs coeff (cm^{-1})	10.60	10.24	7.44	7.31	7.34
cryst size (mm)	0.4 × 0.04 × 0.02	0.4 × 0.35 × 0.03	0.6 × 0.4 × 0.04	0.7 × 0.1 × 0.08	0.5 × 0.4 × 0.3
max θ (deg)	28.51	28.49	28.48	24.00	28.51
index ranges	$-11 \le h \le 8$	$-33 \le h \le 31$	$-11 \le h \le 13$	$-11 \le h \le 11$	$-15 \le h \le 13$
	$-25 \le k \le 23$	$-11 \le k \le 11$	$-15 \le k \le 18$	$-19 \le k \le 20$	$-15 \le k \le 17$
	$-12 \le l \le 16$	$-9 \le l \le 12$	$-17 \le l \le 20$	$-21 \le l \le 19$	$-18 \le l \le 19$
no. of reflns collected	11992	12025	6557	10173	6690
no. of indep reflns	4649	4359	2582	3530	2619
no. of obsd reflns[a]	2561	2864	1547	2125	2173
refinement meth	full-matrix on F^2	full-matrix on F^2	full-matrix on F^2	full-matrix on F^2	full-matrix on F^2
data/restraints/params	4649/0/237	4359/1/192	2582/0/162	3530/20/347	2619/0/140
GOF on F^2	0.932	0.976	1.023	1.017	1.044
final R indices [$I > 2\sigma(I)$]	R1 = 0.0495	R1 = 0.0643	R1 = 0.0681	R1 = 0.0731	R1 = 0.0371
R indices (all data)[b,c]	wR2 = 0.1129	wR2 = 0.1442	wR2 = 0.1876	wR2 = 0.2077	wR2 = 0.1107
wt params a, b	0.0455, 0.0000	0.0710, 0.0000	0.0980, 0.2100	0.1200, 0.0000	0.0678, 0.9564
largest peak/hole (e Å^{-3})	0.387 and −0.448	0.796 and −0.439	0.747 and −0.529	0.881 and −0.632	0.495 and −0.317

[a] $[I > 2\sigma(I)]$. [b] $wR1 = \sum||F_o| - |F_c||/|F_o|$. [c] $wR2 = [[w(F_o^2 - F_c^2)^2]/\sum[w(F_o^2)^2]]^{1/2}$, calc $w = 1/[\sigma^2(F_o^2) + (aP)^2 + bP]$ where $P = (F_o^2 + 2F_c^2)/3$.

rystallized salts), and a pale orange powder. The FAB^+ mass spectrum in acetonitrile (NBA matrix) exhibited a 100% peak at $m/z = 368$ (Mn(L)$(OAc)^+$). The FTIR spectrum (Nujol mull) contains a sharp peak at 3650 cm^{-1}, consistent with known M−OH complexes.[16]

[Mn(1)$(OMe)_2$]PF_6. Mn(**1**)Cl_2 (0.758 g, 0.002 mol) was dissolved in 25 mL of 2 M NaOH, to which 5 mL of EtOH was then added. A dark brown solution resulted. Air was bubbled through the solution overnight. After filtration through Celite to remove traces of brown solids, 1.63 g (0.01 mol) of NH_4PF_6 was added. Immediately, a sticky orange solid precipitated from the solution, which was collected by filtration, washed sparingly with water, and dried in vacuo to give the crude product. Recrystallization by ether diffusion into a methanol solution gave large, dark red crystals of the product, which were manually separated from a light tan coprecipitate. The crystals were suitable for X-ray diffraction. Yield: 0.494 g (47%). Anal. Calcd for $MnC_{16}H_{36}N_4O_2PF_6$: C 37.22%, H 7.03%, N 10.85%, found: C 37.60%, H 6.79%, N 10.95%. The FAB^+ mass spectrum in acetonitrile (NBA matrix) exhibited a strong peak at $m/z = 327$ (Mn(L)(H_2O)).

Physical Methods. Electrochemical experiments were performed on a Princeton Applied Research model 175 programmer and model 173 potentiostat in dry CH_3CN using a locally made cell in an inert atmosphere drybox under N_2. A button Pt electrode was used as the working electrode in conjunction with a Pt-wire counter electrode and a Ag-wire pseudo-reference electrode. Tetrabutylammonium hexafluorophosphate (0.1 M) was the supporting electrolyte in all cases. The measured potentials were referenced to SHE using ferrocene (+0.400 V versus SHE) as an internal standard.

EPR spectra were recorded on a Bruker ESP300E spectrometer operating in the X-band using ~1 mM complex in dry methanol at 77 K. The solutions were saturated with tetrabutylammonium hexafluorophosphate to improve solubility and improve resolution. Electronic spectra were recorded using a Cary model 3 spectrophotometer controlled by a Dell Dimension XPS P133s computer. Magnetic studies were performed on a Johnson Matthey MSB I magnetic susceptibility balance on solid state samples at ambient temperatures. Conductance measurements[17] were obtained with a YSI model 35 conductance meter on 0.001 M complexes at room temperature.

Potentiometric titrations were performed under N_2 at 25.0 °C with an ionic strength of 0.1000 (KNO_3) on a Brinkmann Metrohm 736GP Titrino equipped with a Brinkmann combination electrode. The electrode was standardized by a five-buffer calibration using the Titrino's internal standardization method followed by titration of a standardized strong acid (HNO_3) with a standardized strong base (KOH) after a literature procedure.[18] The strong acid and the strong base solutions were prepared from carbonate-free water and standardized with the Titrino's internal methods. The KOH solution was stored under N_2 to minimize carbonate formation. In a typical titration, ~10 mg of the material to be titrated was placed in 50.0 mL of the supporting electrolyte solution, and ~2 mL of the KOH solution was added to a $p[H^+] > \sim 11$. The resulting solution was titrated to a $p[H^+]$ value between 2 and 3. The data were fit using the program BETA,[19] which is an updated version of a previous program of the same name,[20] using the pK_w found in the strong acid/base titration. For [Mn(**1**)Cl_2]PF_6, 4 replicate titrations were performed, each with a goodness of fit (GOF)[18] < 2.2 and a total of 1904 data points.

Crystal Structure Analysis. X-ray data were collected with a Siemens SMART[21] three-circle system with CCD area detector using graphite-monochromated Mo Kα radiation ($\lambda = 0.71073$ Å). The crystals were held at the specified temperature with the Oxford Cryosystem cooler.[22] Absorption corrections were applied by the Ψ-scan method, and none of the crystals showed any decay during data collection. Complete data for all crystal are shown in Table 1. The structures were solved by direct methods using SHELXS[23] (TREF) with additional light atoms found by Fourier methods. Hydrogen atoms were

(16) Nakamoto, K. *Infrared and Raman Spectra of Inorganic and Coordination Compounds*, 3rd ed.; Wiley: New York, 1978.
(17) (a) Angelici, R. J. *Synthesis and Techniques in Inorganic Chemistry*, 2nd ed.; University Science Books: Mill Valley, CA, 1986, Appendix 2. (b) Feltham, R. D.; Hayter, R. G. *J. Chem. Soc.* **1964**, 4587. (c) Geary, W. J. *Coord. Chem. Rev.* **1971**, *7*, 81.
(18) Turowski, P. N.; Rodgers, S. J.; Scarrow, R. C.; Raymond, K. N. *Inorg. Chem.* **1988**, *27*, 474.
(19) McCormick, J. M.; Raymond, K. N. Unpublished results.
(20) (a) Avdeef, A.; Raymond, K. N. *Inorg. Chem.* **1979**, *18*, 1605. (b) Harris, W. R.; Raymond, K. N. *J. Am. Chem. Soc.* **1979**, *101*, 6534.
(21) SMART User's manual, Siemens Industrial Automation Inc, Madison, WI.
(22) Cosier, J.; Glazer, A. M. *J. Appl. Crystallogr.* **1986**, *19*, 105.
(23) Sheldrick, G. M. *Acta Crystallogr.* **1990**, *A46*, 467.

Table 2. Selected Bond Lengths (Å) and Angles (deg)

(i) For $[Mn(\mathbf{2})Cl_2]PF_6$

Mn1−N11	2.087(3)	Mn1−N110	2.211(3)
Mn1−N17	2.111(3)	Mn1−Cl12	2.2808(10)
Mn1−N14	2.202(3)	Mn1−Cl11	2.3030(10)
N11−Mn1−N17	81.29(11)	N14−Mn1−Cl12	96.32(8)
N11−Mn1−N14	82.73(11)	N110−Mn1−Cl12	100.64(8)
N17−Mn1−N14	78.61(11)	N11−Mn1−Cl11	92.88(8)
N11−Mn1−N110	78.89(11)	N17−Mn1−Cl11	174.11(9)
N17−Mn1−N110	81.98(11)	N14−Mn1−Cl11	99.91(9)
N14−Mn1−N110	155.01(11)	N110−Mn1−Cl11	97.79(9)
N11−Mn1−Cl12	175.36(8)	Cl12−Mn1−Cl11	91.76(4)
N17−Mn1−Cl12	94.07(9)		

(ii) For $[Mn(\mathbf{1})Cl_2]PF_6$

Mn(1)−N(1)	2.115(4)	Mn(1)−N(11)	2.261(6)
Mn(1)−N(8)	2.199(5)	Mn(1)−Cl(1)	2.269(2)
Mn(1)−N(4)	2.229(6)	Mn(1)−Cl(2)	2.327(2)
N(1)−Mn(1)−N(8)	81.7(2)	N(4)−Mn(1)−Cl(1)	90.6(2)
N(1)−Mn(1)−N(4)	82.4(2)	N(11)−Mn(1)−Cl(1)	95.2(2)
N(8)−Mn(1)−N(4)	90.4(2)	N(1)−Mn(1)−Cl(2)	93.1(2)
N(1)−Mn(1)−N(11)	90.9(2)	N(8)−Mn(1)−Cl(2)	170.6(2)
N(8)−Mn(1)−N(11)	81.4(2)	N(4)−Mn(1)−Cl(2)	96.7(2)
N(4)−Mn(1)−N(11)	170.1(2)	N(11)−Mn(1)−Cl(2)	90.9(2)
N(1)−Mn(1)−Cl(1)	170.14(14)	Cl(1)−Mn(1)−Cl(2)	94.60(8)
N(8)−Mn(1)−Cl(1)	91.4(2)		

(iii) For $[Mn(\mathbf{1})(N_3)_3]PF_6$

Mn(1)−N(011)	1.929(4)	Mn(1)−N(4)	2.306(5)
Mn(1)−N(1)	2.099(3)		
N(011)#1−Mn(1)−N(011)	97.7(3)	N(1)−Mn(1)−N(4)	81.7(2)
N(011)−Mn(1)−N(1)#1	170.5(2)	N(011)−Mn(1)−N(4)#1	92.3(2)
N(011)−Mn(1)−N(1)	89.9(2)	N(1)−Mn(1)−N(4)#1	93.3(2)
N(011)−Mn(1)−N(4)	92.1(2)	N(4)−Mn(1)−N(4)#1	173.4(2)

(iv) For $[Mn(\mathbf{1})(OH)(OAc)]PF_6$

Mn(1)−O(1)	1.812(4)	Mn(1)−N(11)	2.157(5)
Mn(1)−O(2)	1.965(4)	Mn(1)−N(1)	2.248(5)
Mn(1)−N(4)	2.110(5)	Mn(1)−N(8)	2.298(6)
O(1)−Mn(1)−O(2)	96.6(2)	N(4)−Mn(1)−N(1)	83.2(2)
O(1)−Mn(1)−N(4)	172.1(2)	N(11)−Mn(1)−N(1)	89.6(2)
O(2)−Mn(1)−N(4)	89.4(2)	O(1)−Mn(1)−N(8)	96.5(2)
O(1)−Mn(1)−N(11)	91.3(2)	O(2)−Mn(1)−N(8)	90.4(2)
O(2)−Mn(1)−N(11)	169.5(2)	N(4)−Mn(1)−N(8)	88.6(2)
N(4)−Mn(1)−N(11)	83.4(2)	N(11)−Mn(1)−N(8)	81.9(2)
O(1)−Mn(1)−N(1)	90.9(2)	N(1)−Mn(1)−N(8)	168.9(2)
O(2)−Mn(1)−N(1)	97.0(2)		

(v) For $[Mn(\mathbf{1})(OMe)_2]PF_6$

Mn(1)−O(1)	1.838(2)	Mn(1)−N(1)	2.344(2)
Mn(1)−N(4)	2.137(2)		
O(1)#1−Mn(1)−O(1)	102.83(10)	O(1)−Mn(1)−N(1)	96.25(7)
O(1)#1−Mn(1)−N(4)	87.78(7)	N(4)−Mn(1)−N(1)	80.45(7)
O(1)−Mn(1)−N(4)	169.05(7)	N(4)#1−Mn(1)−N(1)	89.18(7)
N(4)−Mn(1)−N(4)#1	81.76(8)	N(1)−Mn(1)−N(1)#1	166.31(9)
O(1)#1−Mn(1)−N(1)	92.28(7)		

added at calculated positions and refined using a riding model. Anisotropic displacement parameters were used for all non-H atoms, while H-atoms were given isotropic displacement parameters equal to 1.2 (or 1.5 for methyl hydrogen atoms) times the equivalent isotropic displacement parameter for the atom to which the H atom is attached. Refinement used SHELXL 96.[24] Selected bond lengths and angles for the complexes may be found in Table 2, while all bond lengths and angles, atomic coordinates and equivalent isotropic displacement paramaters, and hydrogen coordinates and isotropic displacement parameters are included in the Supporting Information.

Comments on Specific Crystal Structures. $[Mn(\mathbf{2})Cl_2]PF_6$: crystal character, red needles. Systematic absences indicated space group $P2_1/n$. $[Mn(\mathbf{1})Cl_2]PF_6$: crystal character, red plates. Systematic absences indicated either space group $Pna2_1$ or *Pnma*. The former was chosen because of the value of *Z* and the likely absence of mirror symmetry and shown to be correct by successful refinement. $[Mn(\mathbf{2})(N_3)_2]PF_6$: crystal character, brown laths. Systematic absences indicated either space group *C*2/*c* or *Cc*. The latter was initially chosen for successful structure solution, but inspection of the refined molecule showed that it could be placed in the centrosymmetrical space group with the Mn−ligand cation on a 2-fold axis and the PF_6 on an inversion center. *C*2/*c* was shown to be correct by successful refinement. Disorder was evident in the PF_6 group with minor components for F2 and F3 (occupancies 0.89(1):0.11). A minor component for C9 was also present (occupancies 0.67(1):0.33). The H atoms of the minor component were not included. $[Mn(\mathbf{1})(OH)(OAc)]PF_6$: crystal character, dark brown laths. Systematic absences indicated space group $P2_1/n$. $[Mn(\mathbf{1})(OMe)_2]PF_6$: crystal character, deep red-brown blocks. Systematic absences indicated either space group *C*2/*c* or *Cc*. The former was chosen on the basis of intensity statistics and shown to be correct by successful refinement. However, the structure was solved in *Cc* and then converted to *C*2/*c*. The Mn cation lies on a 2-fold axis and the PF_6 group on a center of inversion.

Results and Discussion

The New Compounds and Their Structures. Previously reported electrochemical studies[13] on these complexes revealed that the trivalent states should be easily accessible through chemical oxidation with relatively mild oxidants. Direct halogen oxidation of the divalent metal complexes in methanol solutions under nitrogen produced the desired result while avoiding the complications associated with hydroxide and oxide ligands. In the presence of excess PF_6^- anion, the addition of excess bromine gave immediate precipitates of the characteristically sparingly methanol soluble PF_6^- salts of the one electron oxidized products, which, surprisingly retained their two chloride ligands. The failure of Br^- to substitute for the chloride ion in this reaction suggests a thermodynamic preference for Cl^- coordination by the relatively hard trivalent metal ions. Other factors favoring this product are the almost immediate precipitation of the hexafluorophosphate salt upon oxidation and the low extent of Cl^- dissociation from the metal ions in methanol solutions (vide infra). The products generally required no further purification and were obtained in high yields.

X-ray quality crystals of the Mn^{3+} complexes of **1** and **2** were obtained by ether diffusion into acetone solutions, and their molecular structures have been determined. Figure 2 displays representations of these molecules. As expected, the cross-bridged tetraazamacrocyclic ligands occupy two cis equatorial and two axial coordination sites, leaving two adjacent sites for the monodentate chloride ligands, in the pseudo octahedral coordination sphere of the metal ion. The short ethylene cross-bridge constrains the parent macrocycle into a folded conformation, which is the same as that preferred by the small unbridged 12-membered macrocyclic ligand cyclen.[25] As is well-known, the parent unbridged 14-membered ligand, cyclam, tends to bind with all four of its donor atoms in a planar array, positioning the monodentate ligands in mutually trans sites.[26,27] The chemical benefits of having two adjacent labile sites (as in the

(24) Sheldrick, G. M., SHELX-96 (beta-test) (including SHELXS and SHELXL), University of Göttingen, 1996.
(25) (a) Henrick, K.; Tasker, P. A.; Lindoy, L. F. *Prog. Inorg. Chem.* **1985**, *33*, 1. (b) Busch, D. H. *Acc. Chem. Res.* **1978**, *11*, 392. (c) Iitaka, Y. S.; Shina, M.; Kimura, E. *Inorg. Chem.* **1974**, *13*, 2886. (d) Collman, J. P.; Schneider, P. W. *Inorg. Chem.* **1966**, *5*, 1380.
(26) (a) Fabbrizzi, L. *Comments Inorg. Chem.* **1985**, *4* (1), 33. (b) Martin, L. Y.; Sperati, C. R.; Busch, D. H. *J. Am. Chem. Soc.* **1977**, *99*, 2968. (c) Martin, L. Y.; Zompa, L. J.; DeHayes, L. J.; Busch, D. H. *J. Am. Chem. Soc.* **1974**, *96*, 4046.
(27) For exceptions, see: (a) Brewer, K. J.; Calvin, M.; Lumpkin, R. S.; Otvos, J. W.; Spreer, L. O. *Inorg. Chem.* **1989**, *28*, 4446. (b) Che, C.-M.; Kwong, S.-S.; Poon, C.-K.; Lai, T.-F.; Mak, T. C. W. *Inorg. Chem.* **1985**, *24*, 1359. (c) Poon. C.-K.; Che, C.-M. *J. Chem. Soc., Dalton Trans.* **1981**, 1336. (d) Lai, T.-F.; Poon, C.-K. *Inorg. Chem.* **1976**, *15*, 1562.

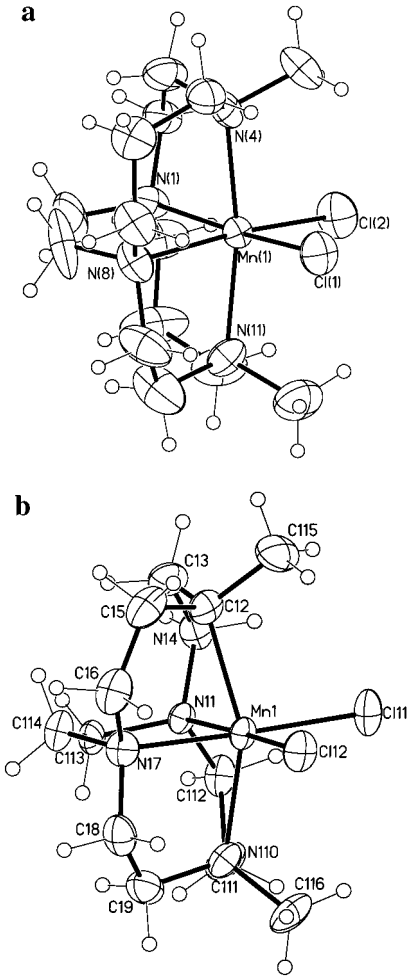

Figure 2. Representations of the crystal structures of (a) Mn(**1**)Cl_2^+ and (b) Mn(**2**)Cl_2^+. Crystal data are given in Table 1, selected bond lengths and angles may be found in Table 2, and atomic coordinates are collected in Tables 3 and 4.

complexes of **1** and **2**) have been discussed in relation to various catalytic and biomimetic processes.[28] As is the case with other metal ions,[13,29] ring size dictates the distortion of the Mn^{3+} complexes from ideal octahedral geometry. The two additional carbon atoms in the parent ring of **1** allow the needed flexibility that allows this ligand to encompass the Mn^{3+} ion more completely. Paradoxically, the smaller, more rigid ligand **2** does remain bound to metal ions[29] under harsh conditions as long as the more flexible ligand **1**. Ligand **2** cannot provide the maximal coordination geometry (octahedral) for the metal ion, illustrating the necessity for good complementarity in order to reap the harvest of increased rigidity in a ligand.

Metrical parameters consistent with Jahn−Teller distortions are seen for both complexes. For Mn(**2**)Cl_2^+, the axial Mn−N_{ax} bond lengths are 2.202(3) and 2.211(3) Å while equatorial Mn−N_{eq} bond lengths are 2.087(3) and 2.111(3) Å, a difference of over 0.1 Å, on average, between axial and equatorial bond lengths. For Mn(**1**)Cl_2^+, a similar distortion is also clear, with

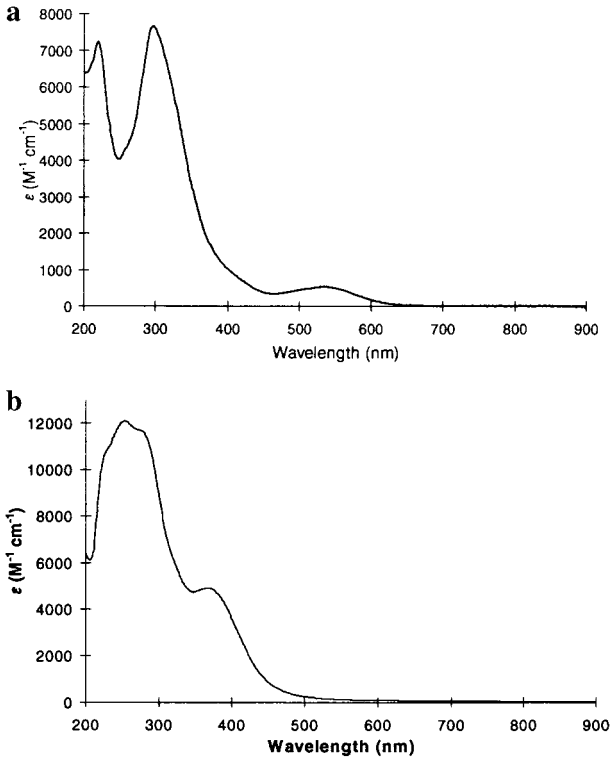

Figure 3. The electronic spectra of (a) [Mn(**1**)Cl_2]PF_6 and (b) [Fe(**1**)Cl_2]PF_6 in acetonitrile. The spectra of [Mn(**2**)Cl_2]PF_6 and [Fe(**2**)Cl_2]PF_6 are quite similar, respective of metal ion, and are, therefore, not pictured.

an average difference of just less than 0.09 Å. Since Mn^{3+} is a d^4 ion, Jahn−Teller distortions are expected, but the noncubic symmetries enforced by the cross-bridged ligands might have been expected to remove the degeneracy that leads to the Jahn−Teller distortion in the first place.

The electronic structures of the new compounds are reflected in their magnetic moments, μ_{eff}, which were obtained at ambient temperatures on solid samples and are typical of high-spin d^4 ions in the case of manganese(III) and d^5 ions for iron(III):[30] $\mu_{eff} = 5.00\ \mu_B$ for [Mn(**1**)Cl_2]PF_6 and 4.87 μ_B for [Mn(**2**)Cl_2]PF_6; $\mu_{eff} = 5.95\ \mu_B$ for [Fe(**1**)Cl_2]PF_6 and 5.90 μ_B for [Fe(**2**)Cl_2]PF_6. These results are consistent with the fact that dimerization, common to higher valent synthetic complexes of both iron[31] and manganese[32] under oxidizing conditions, does not occur in the preparation of bulk solid samples of the new complexes of these trivalent metal ions. Such dimers commonly have reduced magnetic moments due to antiferromagnetic interactions between the pairs of metal ions, although this observation alone is not a definitive structure proof.

The electronic spectra of these complexes, as illustrated for the Fe^{3+} and Mn^{3+} complexes of ligand **1** in Figure 3, exhibit several charge transfer bands,[33] and a complete listing of absorption bands is found in Table 3. These spectra have been used as probes in studying the reactivity of the complexes in harsh media by UV−vis spectroscopic methods.[34]

(28) (a) Alexander, M. D.; Busch, D. H. *J. Am. Chem. Soc.* **1966**, *88*, 1130. (b) Chin, J.; Banaszczyk, M.; Jubian, V.; Zou, X. *J. Am. Chem. Soc.* **1989**, *111*, 186. (c) Hettich, R.; Schneider, H.-J. *J. Am. Chem. Soc.* **1997**, *119*, 5638. (d) Arciero, D. M.; Lipscomb, J. D. *J. Biol. Chem.* **1986**, *261*, 2170. (e) Halfen, J. A.; Mahapatra, S.; Wilkinson, E. C.; Kaderli, S.; Young, V. G., Jr.; Que, L., Jr.; Zuberbühler, A. D.; Tolman, W. B. *Science* **1996**, *271*, 1397. (f) Ross, P. K.; Solomon, E. I. *J. Am. Chem. Soc.* **1991**, *113*, 3246.

(29) Hubin, T. J.; McCormick, J. M.; Alcock, N. W.; Busch, D. H. In preparation.

(30) Huheey, J. E.; Keiter, E. A.; Keiter, R. L. *Inorganic Chemistry: Principles of Structure and Reactivity*, 4th ed.; Harper Collins: New York, 1993; p 463.

(31) Murray, K. S. *Coord. Chem. Rev.* **1974**, *12*, 1.

(32) (a) Wieghardt, K. *Angew. Chem., Int. Ed. Engl.* **1989**, *28*, 1153. (b) Brudvig, G. W.; Crabtree, R. H. *Prog. Inorg. Chem.* **1989**, *37*, 99. (c) Law, N. A.; Caudle, T.; Pecoraro, V. L. In *Advances in Inorganic Chemistry*; Sykes, A. G., Ed.; Academic Press: New York, 1999; Vol. 46, p 305.

(33) Lever, A. B. P. *Inorganic Electronic Spectroscopy*, 2nd ed.; Elsevier: Amsterdam, 1984.

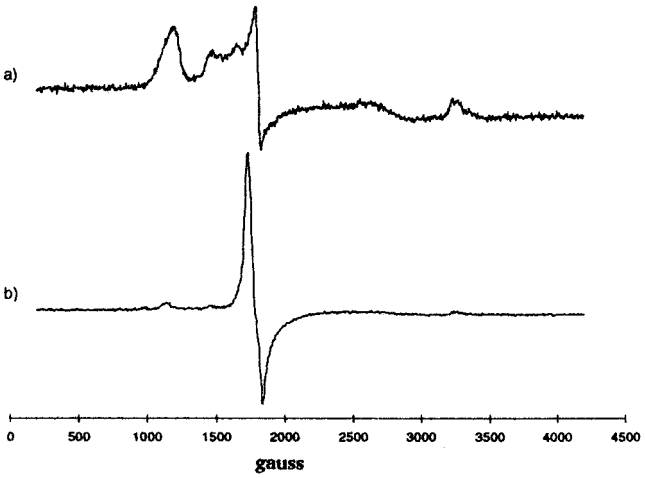

Figure 4. X-band EPR spectra of (a) [Fe(**2**)Cl_2]PF_6 and (b) [Fe(**1**)-Cl_2]PF_6 (1 mM solutions in methanol saturated with tetrabutylammonium hexafluorophosphate at 77 K).

Table 3. Electronic Spectra of Trivalent Dichloro Complexes in Acetonitrile

complex	λ_{max} (nm)	ϵ (M^{-1} cm^{-1})
[Mn(**1**)Cl_2]PF_6	220	7230
	297	7670
	534	540
[Fe(**1**)Cl_2]PF_6	254	12100
	369	4920
[Mn(**2**)Cl_2]PF_6	219	4790
	294	4070
	530	190
[Fe(**2**)Cl_2]PF_6	281	5990
	399	1580

The high-spin d^5 Fe^{3+} complexes of both **1** and **2** exhibit EPR spectra in methanol at 77 K, Figure 4, while the corresponding Mn^{3+} complexes are EPR silent at 77 K, as expected for high-spin $S = 2$ systems.[35] A large signal near $g = 4.3$ is apparent for both iron(III) complexes. Also observable are peaks near $g = 2.0$ and $g = 6.0$, although these signals have variable intensities. For [Fe(**1**)Cl_2]PF_6, the latter signals have very low intensity compared to the large signal near $g = 4.3$. This is consistent with an approximate rhombic geometry. For [Fe(**2**)Cl_2]PF_6, the signals near $g = 2.0$ and $g = 6.0$ have intensities very nearly the same as the $g = 4.3$ signal, indicating the presence of two types of Fe^{3+}, rhombic and axial,[35] under the conditions of the measurement.

Solution Properties. The results of conductance experiments (Table 4) correlate with the dielectric constant and hydrogen-bonding abilities of the solvents. In low-dielectric solvents with little ability to hydrogen bond, like nitromethane and acetonitrile, only the PF_6^- anion dissociates and the dichloro complexes behave as 1:1 electrolytes, indicating that the structure of the complex in solution is essentially the same as in the solid state. In a coordinating solvent with a similar dielectric constant but more hydrogen-bonding ability, methanol, the iron(III) complexes still behave as 1:1 electrolytes while both manganese(III) complexes now exhibit 2:1 electrolyte behavior, as one chloride is displaced by solvent. This difference must be explained by a combination of a higher thermodynamic affinity of the Fe^{3+} complexes for Cl^- and by the lability of the d^4 ion, Mn^{3+}. Remarkably, in water the electrolytic behavior of all four

Table 4. Molar Conductivities of the 0.001 M Complexes in Several Solvents[a]

	conductance of 0.001 M soln			
complex	nitromethane	acetonitrile	methanol	water
[Fe(**1**)Cl_2]PF_6	87.0	140	122	591
[Fe(**2**)Cl_2]PF_6	90.0	145	109	531
[Mn(**1**)Cl_2]PF_6	91.4	135	203	499
[Mn(**2**)Cl_2]PF_6	99.6	122	187	541
1:1	75−95	120−160	80−115	118−131
2:1	150−180	220−300	160−220	235−273
3:1	220−260	340−420		408−435
4:1	290−330			∼560

[a] Literature values taken from ref 16.

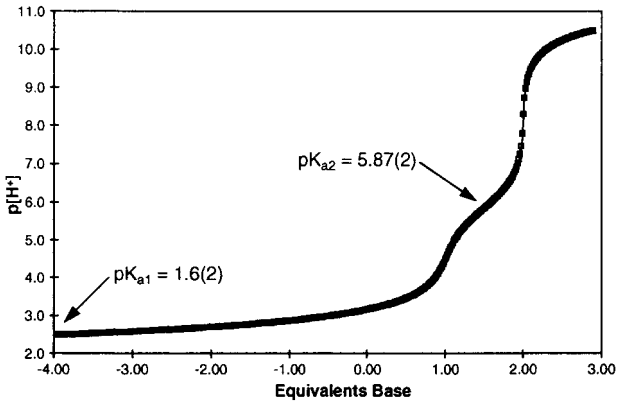

Figure 5. Titration data for [Mn(**1**)Cl_2]PF_6 plotted against equivalents of base calculated per mole of [Mn(**1**)Cl_2]PF_6. The line through the data is the best fit of the data as found by BETA as described in the text.

complexes is consistent with that normally exhibited by 4:1 electrolytes, indicating that, in addition to replacement of both chlorides water molecules, at least one water molecule undergoes substantial deprotonation.

The kinetic stability of the binding between manganese and the bridged macrocycle in [Mn(**1**)Cl_2]PF_6 facilitates measurement of the acidity of its bound water molecules by pH titration in aqueous solution. This conclusion is supported by the fact that satisfactory fits (GOF > 5) cannot be achieved for models that include metal/ligand stability constants in the data treatment. Also, no precipitation of insoluble metal hydroxides is observed at high p[H^+] during the titration, indicating that the concentration of the free metal ion must be extremely small. The titration data for [Mn(**1**)Cl_2]PF_6 (Figure 5) can be fit very well by treating the compound as a weak diprotic acid. The above conductance measurements suggest that both chlorides are replaced by water in aqueous solution; further, both water molecules have pK_a's in the accessible p[H^+] region. The pK_a for the first bound water is 1.6(2), which is consistent with the known Lewis acidity of the Mn^{3+} ion (the first two pK_a's for $Mn(H_2O)_6^{3+}$ are 0.82 and 0.94, respectively)[36] and with the aqueous conductance data. The second bound water for [Mn(**1**)$(OH_2)_2$]$^{3+}$ is deprotonated with pK_a = 5.87(2). The similarity of the pK_{a1} values of the bridged cyclam derivative and the hydrated metal ion suggests that the great stability of the complex arises from topological and rigidity effects, not from extreme electronic effects. With the electron density comparable to that of the hydrated metal ion, the complex might be expected to exchange its two water molecules at a rate similar to that of hydrated manganese(III).

(34) Bucholova, M.; Hubin, T. J.; McCormick, J. M.; Busch, D. H. In preparation.
(35) Drago, R. S. *Physical Methods for Chemists*, 2nd ed.; Saunders College Publishing: Ft. Worth, 1992.
(36) Martell, A. E.; Smith, R. M.; Motekaitis, R. J. *NIST Standard Reference Database 46, Version 2.0*; NIST Standard Reference Data: Gaithersberg, MD, 1995.

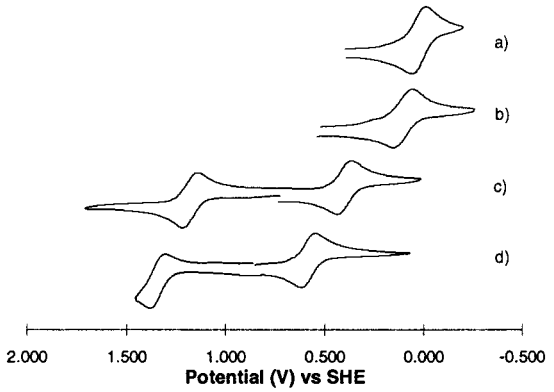

Figure 6. Cyclic voltammograms for (a) [Fe(**2**)Cl_2]PF_6, (b) [Fe(**1**)Cl_2]PF_6, (c) [Mn(**2**)Cl_2]PF_6, and (d) [Mn(**1**)Cl_2]PF_6 in acetonitrile.

Table 5. Redox Potentials (vs SHE) for the Complexes with Peak Separations

complex	redox couple	$E_{1/2}$ (V)	($E_a - E_c$) (mV)
[Fe(**2**)Cl_2]PF_6	Fe^{3+}/Fe^{2+}	+0.026	60
[Fe(**1**)Cl_2]PF_6	Fe^{3+}/Fe^{2+}	+0.106	79
[Mn(**2**)Cl_2]PF_6	Mn^{3+}/Mn^{2+}	+0.400	71
	Mn^{4+}/Mn^{3+}	+1.177	76
[Mn(**1**)Cl_2]PF_6	Mn^{3+}/Mn^{2+}	+0.582	72
	Mn^{4+}/Mn^{3+}	+1.343	76

The electrolyte type in aqueous media, the great kinetic stability of the complex, and, as pointed out above, the rapid substitution rates at the monodentate binding sites all support the prediction that the complex will be capable of surviving in relatively harsh catalysis media.

The cyclic voltammograms of the complexes in acetonitrile are shown in Figure 6, and the redox potentials and peak separations, in Table 5. These rigid ligands stabilize a range of oxidation states for manganese, from Mn^{2+} to Mn^{4+} as shown by the two pseudo-reversible redox couples of [Mn(**1**)Cl_2]$^+$ and [Mn(**2**)Cl_2]$^+$. In contrast, only the Fe^{3+}/Fe^{2+} couple is observed for [Fe(**1**)Cl_2]$^+$ and [Fe(**2**)Cl_2]$^+$. From this perspective the manganese complexes are very likely to function as oxidation catalysts with a variety of terminal oxidants. Indeed, the compounds are of interest to technology.[37] Also of note is the ring size effect between the metal ion derivatives of 14-membered **1** and 12-membered **2**. The smaller ring complexes are consistently easier to oxidize, which may be explained simply on the basis of size; the smaller cavity better stabilizes the smaller oxidized metal ion.

Additional Unusual Mn(1)$^{3+}$ Complexes. The unique properties of the dichloro complex of Mn^{3+} and ligand **1**, especially its impressive stability under harsh aqueous conditions and its utility as an aqueous oxidation catalyst,[37] motivated the further study of this species. Of special significance are the reactivity at the labile cis sites and the identification of potential intermediates for catalytic cycles in aqueous media. Three additional Mn^{3+} complexes with **1** have been synthesized and characterized by X-ray crystal structure determination, and all are of interest from that perspective. These compounds are [Mn(**1**)$(N_3)_2$]PF_6, [Mn(**1**)(OH)(OAc)]PF_6, and [Mn(**1**)$(OMe)_2$]PF_6, and representations of them appear in Figure 7. For all three compounds, the $N_{eq}-Mn-N_{eq}$ and $N_{ax}-Mn-N_{ax}$ bond angles are not significantly different from those of Mn(**1**)Cl_2^+, as described earlier, indicating that the Mn^{3+} ion occupies a relatively complementary cavity within ligand **1**. Selected bond lengths and angles are listed in Table 2. The bis-azido complex has almost linear azide ligands, with N(011)−N(012)−N(013) = 177.7(7)°.

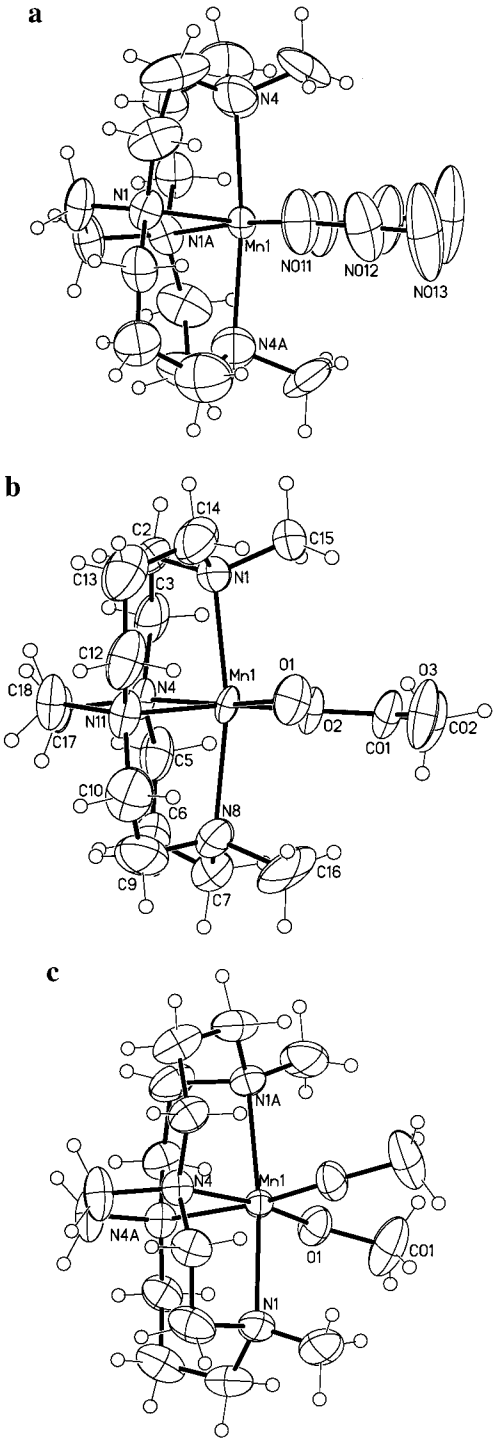

Figure 7. Crystal structures of (a) [Mn(**1**)$(N_3)_2$]PF_6, (b) [Mn(**1**)(OH)(OAc)]PF_6, and (c) [Mn(**1**)$(OMe)_2$]PF_6. Crystal data are given in Table 1, selected bond lengths and angles may be found in Table 2, and atomic coordinates are collected in Tables 5 and 7.

The most interesting of these structures is the hydroxo complex Mn(**1**)(OH)(OAc)$^+$. This is only the third structurally characterized monomeric manganese(III) hydroxo complex.[38]

(37) (a) Busch, D. H.; Collinson, S. R.; Hubin, T. J. Catalysts and Methods for Catalytic Oxidation. WO 98/39098, Sept 11, 1998. (b) Busch, D. H.; Collinson, S. R.; Hubin, T. J.; Labeque, R.; Williams, B. K.; Johnston, J. P.; Kitko, D. J.; Burkett-St. Laurent, J. C. T. R.; Perkins, C. M. Bleach Compositions. WO 98/39406, Sept 11, 1998.

(38) (a) Shirin, Z.; Young, V. G.; Borovik, A. S. *Chem. Commun. (Cambridge)* **1997**, 1967. (b) Eichorn, D. M.; Armstrong, W. H. *J. Chem. Soc., Chem. Commun.* **1992**, 85.

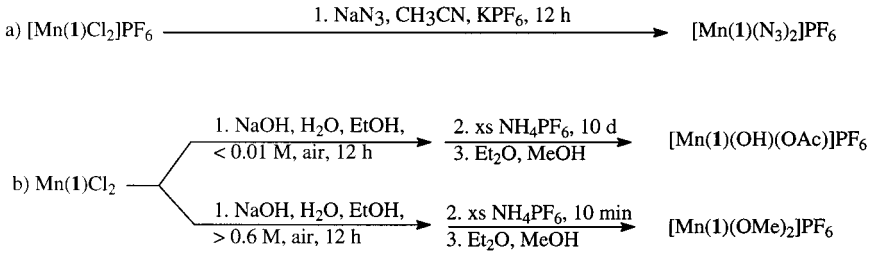

Figure 8. Preparation of (a) $[Mn(\mathbf{1})(N_3)_2]PF_6$ from $[Mn(\mathbf{1})Cl_2]PF_6$ and (b) $[Mn(\mathbf{1})(OH)(OAc)]PF_6$ and $[Mn(\mathbf{1})(OMe)_2]PF_6$ from $Mn(\mathbf{1})Cl_2$.

The pertinent metrical parameters are, for the hydroxyl group, Mn(1)−O(1) = 1.812(4) Å and, for the acetate group, Mn(1)−O(2) = 1.965(4) Å; the interatomic distance between O(1) and O(3) is 2.766 Å. The Mn−hydroxo bond length is consistent with those of the other two monuclear manganese(III)−OH structures[38] (1.816(4) and 1.827(3) Å), but is slightly shorter than either and much shorter than the Mn−O(acetate) bond. Since ligand **1** is neutral, the slightly shorter bond length may be electrostatic in origin, in view of the multiple negative charges of the polydentate ligands in the other Mn^{3+}−OH cases. The carbonyl oxygen of the bound acetato ligand is only 2.766 Å away from the hydroxo oxygen, suggesting that a hydrogen bond may stabilize the hydroxo ligand in this structure. One other $Mn^{III}(OH)$ moiety is also stabilized by hydrogen bonding, although the linkages are intermolecular, between pairs of $Mn^{III}(OH)$ molecules.[38b]

The labilities of the two chloro ligands in $Mn(\mathbf{1})Cl_2^+$ were probed by simple ligand metathesis reactions. Qualitatively, several monodentate, monoanionic ligands replace chloride if present in excess in acetonitrile solutions. Illustrative of this reactivity, the bis-azido complex (Figure 8a) was prepared in high yield (77%) and gave X-ray quality crystals (ether diffusion into a methylene chloride solution). This reaction shows that the chloro ligands are relatively labile in acetonitrile solution and that the occupancy of the labile cis coordination sites should be easily manipulated for other purposes. The bis-azido complex has properties similar to those of the dichloro complex (vide infra).

Two additional $Mn(\mathbf{1})^{3+}$ complexes were obtained from reactions under aqueous conditions. It is well-known that synthetic manganese complexes combine into dimeric or polymeric oxo-bridged species in oxygenated basic aqueous solutions,[32] which commonly involve diamond-shaped dimanganese−bis-(μ-oxo) core units. However, Cache molecular modeling studies indicated that the methyl groups protruding from the two nonbridgehead ligand nitrogens should interfere with such dimerization of the present manganese complexes. Models show that this type of oxygen bridging would place the methyl groups of both ligands in approximately the same locations in space. To test for the formation of dimers, as well as to test the stability of the complex under strongly basic conditions, the manganese(II) complex, $Mn(\mathbf{1})Cl_2$,[13] was dissolved in a 5:1 water:ethanol solution containing 2 M NaOH, and air was bubbled through the solution overnight. Oxidation to Mn^{3+} is seemingly very fast, as the nearly colorless starting material gives a golden brown solution almost immediately. No clear evidence of dimerization was found; i.e., neither the characteristic green color nor the 16-line EPR spectrum[32] associated with the common bis(μ-oxo) $Mn^{III/IV}$ dimer was seen,[39] although this does not rule out the presence of $Mn^{III/III}$ or $Mn^{IV/IV}$ dimers. Filtration of the present solution removed trace brown solids (probably MnO_2 from trace Mn_{aq}^{2+} impurities), after which excess NH_4PF_6 was added to the solution to precipitate PF_6^- salts.

The product isolated at this point depends on the precise reaction conditions (Figure 8b). At low (<0.01 M) concentrations, precipitation occurs slowly over the course of several days to yield thin orange plates of a mixed salt, containing a rare mononuclear manganese(III) hydroxide complex, $[Mn(\mathbf{1})(OH)(OAc)]^+$.[38] Such species have recently been implicated as intermediates in O_2 production from the oxygen-evolving complex of photosynthesis.[40] Intriguingly, the acetate ligand, which helps stabilize the hydroxo complex through an intramolecular hydrogen bond (vide supra), must be produced in situ by oxidation of the ethanol cosolvent, almost certainly, by some $Mn(\mathbf{1})^{n+}$ oxidant. Discounting the unlikely degradation of ligand **1**, no other source of acetate ions is available, because only chloride and PF_6^- salts have been introduced to the system. Other studies have shown $Mn(\mathbf{1})Cl_2$ to be a relatively poor catalyst for the oxidation of alcohols, but it does display some turnover.[34] A slow catalytic reaction would also explain the very slow, steady precipitation of the product over the course of several days.

If the above reaction is carried out at high concentrations (> 0.6 M), an immediate precipitate of a sticky orange powder is formed upon addition of ammonium hexafluorphosphate. Ether diffusion into a methanol solution of this crude product gives dark red crystals of $[Mn(\mathbf{1})(OMe)_2]PF_6$, along with a pale orange coprecipitate. Again, since no methanol or methoxy anion is present in the original reaction mixture, it is likely that the uncharacterized original product reacts with the methanol solvent during recrystallization to give the dimethoxy product. From the chloride replacement reactions, titration data, and the structure of the monohydroxo complex, it is logical to suggest a dihydroxo derivative of $Mn(\mathbf{1})^{3+}$ as the likely intermediate in the formation of the dimethoxy complex. The same species is probably present in the reaction conducted at low concentrations, but for solubility reasons, only the acetato−monohydroxo product is isolated. In contrast, at higher concentrations of complex the PF_6^- salt of the dihydroxo complex precipitates before ethanol can be oxidized to acetate. Efforts are continuing to isolate this putative dihydroxo complex for further characterization.

The electronic properties of these additional $Mn(\mathbf{1})^{3+}$ complexes have been briefly probed using electronic spectroscopy and cyclic voltammetry. The electronic spectra of $[Mn(\mathbf{1})(N_3)_2]^+$, $[Mn(\mathbf{1})(OH)(OAc)]^+$, and $[Mn(\mathbf{1})(OMe)_2]^+$ in acetonitrile are shown in Figure 9 and summarized in Table 6. The azide

(39) The bis(μ-oxo) dimer is, however, isolated from similar reactions of the Mn^{2+} complex of a similar cross-bridged ligand where the methyl groups have been replaced by hydrogens.[29]

(40) Hoganson, C. W.; Lydakis-Simantiris, N.; Tang, X.-S.; Tommos, C.; Warncke, K.; Babcock, G. T.; Diner, B. A.; McCracken, J.; Styring, S. *Photosynth. Res.* **1995**, *46*, 177.

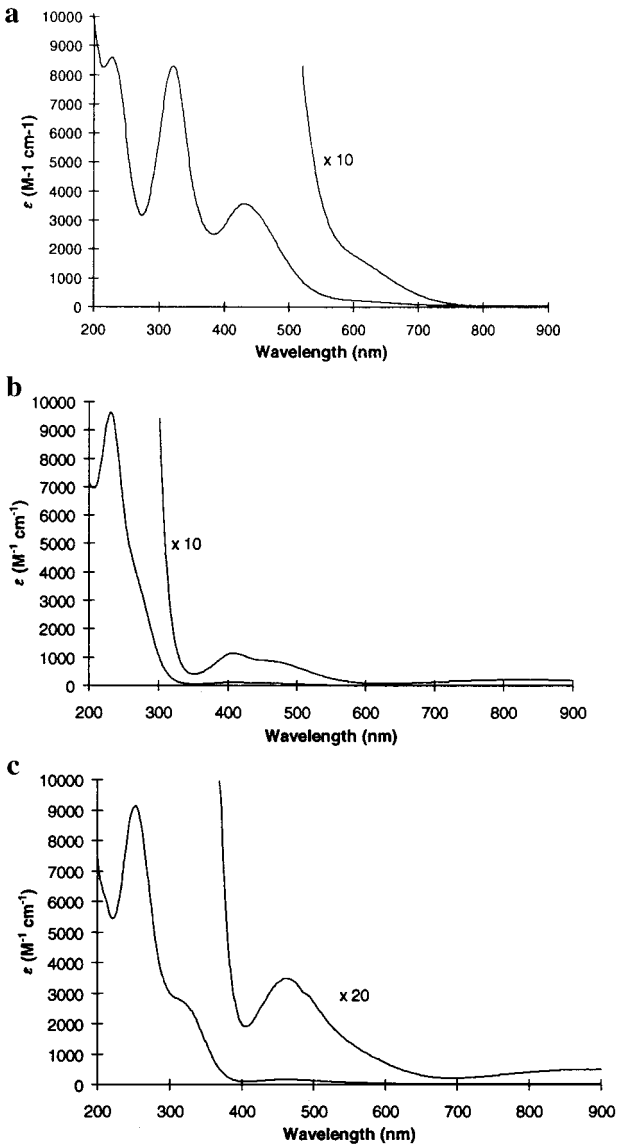

Figure 9. Electronic spectra of (a) [Mn(**1**)$(N_3)_2$]PF_6, (b) [Mn(**1**)(OH)(OAc)]PF_6, and (c) [Mn(**1**)$(OMe)_2$]PF_6 in acetonitrile.

Table 6. Electronic Spectra of $Mn(1)^{3+}$ Complexes in MeCN

complex	λ_{max} (nm)	ϵ (M^{-1} cm^{-1})
[Mn(**1**)$(N_3)_2$]PF_6	227	8600
	321	8310
	433	3570
	625	170
[Mn(**1**)(OH)(OAc)]PF_6	231	9640
	409	110
	478 (sh)	80
[Mn(**1**)$(OMe)_2$]PF_6	252	9140
	324 (sh)	2600
	464	170

complex has an electronic spectrum very similar in appearance to that of the dichloride complex (Figure 3, Table 3), except that the wavelength and the extinction coefficient of the lowest energy charge transfer band is much different, an observation that is not unusual for charge-transfer bands when changing the nature of the ligand (azide for chloride). The spectra of the acetato−hydroxo and dimethoxy complexes are distinctly different from that of the dichloride complex, while strongly resembling each other. Only one very strong charge-transfer band is seen at high energy for these two complexes, while the

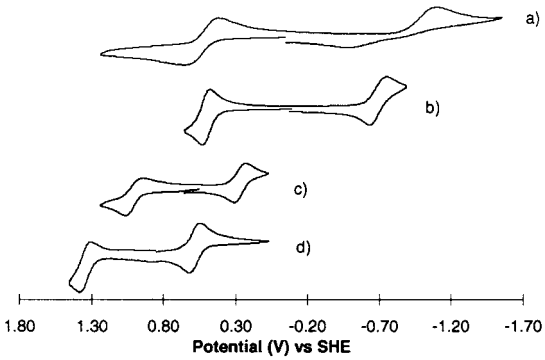

Figure 10. Cyclic voltammograms for (a) [Mn(**1**)$(OMe)_2$]PF_6, (b) [Mn(**1**)(OH)(OAc)]PF_6, (c) [Mn(**1**)$(N_3)_2$]PF_6, and (d) [Mn(**1**)Cl_2]PF_6 in acetonitrile.

Table 7. Redox Potentials (vs SHE) for $Mn(1)^{3+}$ Complexes with Peak Separations

complex	redox couple	$E_{1/2}$ (V)	$(E_a - E_c)$ (mV)
[Mn(**1**)Cl_2]PF_6	Mn^{3+}/Mn^{2+}	+0.582	72
	Mn^{4+}/Mn^{3+}	+1.343	76
[Mn(**1**)(N_3)]PF_6	Mn^{3+}/Mn^{2+}	+0.269	81
	Mn^{4+}/Mn^{3+}	+1.005	118
[Mn(**1**)(OH)(OAc)]PF_6	Mn^{3+}/Mn^{2+}	−0.689	132
	Mn^{4+}/Mn^{3+}	+0.505	62
[Mn(**1**)$(OMe)_2$]PF_6	Mn^{3+}/Mn^{2+}	−0.781	628
	Mn^{4+}/Mn^{3+}	+0.542	243

dichloride and bis-azido complex exhibit two such bands. In addition, these complexes with oxygen ligands have a somewhat resolved band at lower energy whose extinction coefficient is consistent with d−d transitions, but whose energy appears too high for that assignment.[33]

The cyclic voltammograms (Figure 10, Table 7) of the four $Mn(1)^{3+}$ complexes show much greater differences in behavior. The azide complex displays Mn^{3+}/Mn^{2+} and Mn^{4+}/Mn^{3+} couples that are similar in reversibility to those of the chloride complex, but the $E_{1/2}$ potentials of these waves are about 300 mV less positive (Figure 10c,d). The hydroxo−acetato complex is even more drastically affected in its redox potentials. In this complex, the Mn^{3+}/Mn^{2+} wave has been displaced to a potential that is quite negative, −0.689 V, and the Mn^{4+}/Mn^{3+} wave is now only +0.505 V positive from SHE (Figure 10b). This is an easily achievable potential with common oxidants and, along with the aqueous titration data, helps explain why the parent complex is a useful aqueous oxidation catalyst.[37] For the diaqua−manganese(III) complex in water, the titration data shows that at least one hydroxo group is present in the coordination sphere at most relevant pH values ($pK_{a1} = 1.6(2)$) and two hydroxo groups are present under basic conditions ($pK_{a2} = 5.87(2)$). If the dihydroxo complex has oxidation potentials similar to those of the hydroxo−acetato analogue, then oxidation to higher metal oxidation states should be relatively easy, facilitating mild oxidations of substrates by high-valent metal-centered intermediates. A similar effect is found for the dimethoxy complex (Figure 10a). Though much less reversible, probably due to the dissociation of methoxide upon reduction, the Mn^{3+}/Mn^{2+} potential is even more negative than that of the hydroxo complex, at −0.781 V. The Mn^{4+}/Mn^{3+} potential is just slightly more positive than that of the acetato−hydroxo derivative, at +0.542 V. These observations, all made in acetonitrile solutions, provide a basis for qualitative prediction of the pH dependence of the redox potentials of the manganese complexes in water. Clearly the very strong electron-donor capacity of the coordinated hydroxo

group moves the potentials to more cathodic values. This suggests that the Mn^{4+} complexes will become less powerful oxidizing agents at higher pH, thereby offering promise of selectivity as a function of pH.

Acknowledgment. The funding of this research by the Procter and Gamble Company is gratefully acknowledged. T.J.H. thanks the Madison and Lila Self Graduate Research Fellowship of the University of Kansas for financial support. We thank EPSRC and Siemens Analytical Instruments for grants in support of the diffractometer. The Kansas/Warwick collaboration has been supported by NATO.

Supporting Information Available: Tables of bond distances and angles, anisotropic displacement parameters, and hydrogen coordinates and isotropic displacement parameters for [Mn(**2**)Cl_2]PF_6, [Mn(**1**)Cl_2]PF_6, [Mn(**1**)$(N_3)_2$]PF_6, [Mn(**1**)(OH)(OAc)]PF_6, and [Mn(**1**)$(OMe)_2$]PF_6. This material is available free of charge via the Internet at http://pubs.acs.org.

IC9912225